10.1109/ULTSYM.2015.0324

A Sub-Nyquist Analog Front-End with Subarray Beamforming for Ultrasound Imaging

Jonathon Spaulding*, Yonina C. Eldar†, Boris Murmann*
* Stanford University, Dept. of Electrical Engineering, Stanford, CA
† Technion – Israel Institute of Technology, Dept. of Electrical Engineering, Haifa, Israel

***Abstract*—Traditional ultrasound imagers suffer from a large data rate between their analog-to-digital converter (ADC) front-end and digital beamforming backend. This high aggregate data rate (typically exceeding 30 Gb/s) is holding back the design of imagers with high transducer counts, such as 2D imaging arrays. Prior work has demonstrated sub-Nyquist sampling techniques in software, which take advantage of the low innovation rate to sample well below the physical bandwidth of the signal. This work demonstrates a PCB-based hardware implementation of a 32-channel analog front-end (AFE) employing sub-Nyquist sampling. We additionally demonstrate a mixer-based subarray beamforming technique that exploits the narrowband nature of the receiver to beamform received signals prior to digitization. Together, these techniques reduce the aggregate data rate by a factor of 43x when compared to a conventional system.**

Keywords—Sub-Nyquist Sampling, Subarray Beamforming, Compressed Sensing, Ultrasound Imaging

I. Introduction

Conventional ultrasound imaging systems use an array of transducer elements to transmit acoustic energy and to receive reflections caused by structural differences within the imaging target [1]. Traditionally, each receiving element uses a dedicated chain of receive electronics, including a low-noise amplifier (LNA), a variable gain amplifier (VGA) to equalize for depth-based attenuation, an anti-aliasing filter (AAF), and a dedicated analog to digital converter (ADC). The ADC often samples at a rate many times higher than the Nyquist rate of the signal to achieve the timing resolution required for the digital beamforming backend. The data rate of such an architecture is thus directly proportional to the physical bandwidth of the transducer, as well as the number of transducers used. In applications with high transducer element counts, such as those using 2D arrays, the aggregate data rate becomes difficult to manage efficiently.

One method to reduce data rates in 2D arrays has been to use sparse arrays either with fixed-pattern or random transducer placements [2-4]. While this technique helps reduce the data rate, it does so at the cost of reducing the receive element count, resulting in a degradation of both beam focus as well as system signal-to-noise ratio (SNR).

An alternative approach to reducing data rates in ultrasound imagers centers around sampling at the rate of innovation. By pre-filtering and digitizing a fraction of the physical receive signal bandwidth, compressive sensing (CS) techniques can be applied to recover a full-rate signal from the low-rate samples [6-8]. This work demonstrates a hardware implementation of a 32-channel sub-Nyquist sampling AFE architecture that was inspired by the work in [5-8]. The architecture of our AFE is presented in Figure 1. As in a conventional ultrasound machine, each active channel has a chain of receive electronics consisting of a high-voltage protection switch, a high-bandwidth LNA, and a VGA. At this point, our architecture differs from that of a conventional receiver in two ways. First, we filter the signal prior to digitization; this filter has a cutoff frequency far below the physical bandwidth of the received signal. Second, we use the narrowband nature of the filtered signal to implement a mixer-based subarray beamforming technique as presented in [9]. The subarray-beamformed signals are sampled at a low-rate, and digitally beamformed in the frequency domain as in [6]. Together, these architectural changes allow for a reduction in both digitizer count as well as overall data rate.

The remainder of this paper is structured as follows. Section II introduces the AFE architecture as well as the overall system architecture used for testing. Section III presents measurement results validating our mixer-based subarray beamforming technique. Section IV presents measurements comparing the performance of our sub-Nyquist sampling AFE to a commercial ultrasound imaging system. Conclusions are presented in Section V.

II. Sub-Nyquist Sampling Architecture

A. Analog Front-End Architecture

Our 32-channel sub-Nyquist sampling AFE was built using discrete components, a photo of the implemented AFE is shown in Figure 2. For testing, the 32 channels are separated into 4

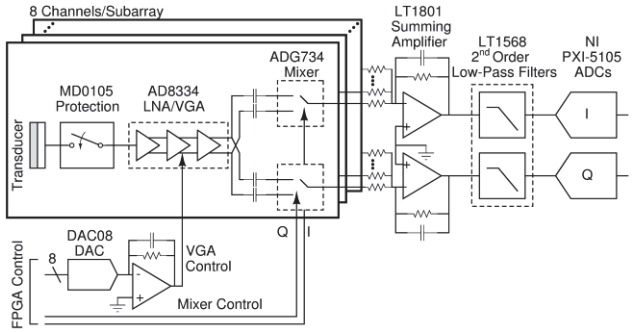

Figure 1: Subarray architecture for sub-Nyquist sampling AFE. 8 channels are beamformed using mixer-based beamforming and summed prior to digitization.

This work was supported in part by Texas Instruments and the Systems on Nanoscale Information fabrICs (SONIC), one of the six STARnet Centers, sponsored by MARCO and DARPA.

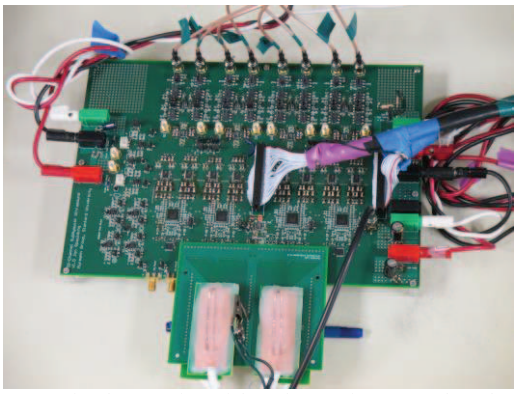

Figure 2: PCB implementation of the sub-Nyquist AFE. The sub-Nyquist AFE measures 7.5x10.8 inches in size, and implements 32 receiving channels.

subarrays of 8 elements each. The architecture for a single subarray is illustrated in Figure 1. MD0105 passive switches protect the LNA from the high voltage transmit pulses. The LNA and VGA blocks are implemented using the AD8334, a 4-channel ultrasound receiver. A single DAC08 8-bit DAC drives the gain control for each AD8334, with a filter to limit out-of-band noise. The differential outputs of each AD8334 channel are mixed in the current domain using an AD734 SPDT switch. Each of the in-phase and quadrature branches within a subarray are summed in the analog domain at the inverting node of an LT1801 amplifier. Finally, the in-phase and quadrature branches of each subarray are filtered using the LT1568, which provides a matched pair of 2nd order Butterworth low-pass filters. Board programmability was added to allow subarray sizes of 4, 8, and 16 elements, as well as filter cutoff frequencies of 365 kHz, 625 kHz, and 1.27 MHz.

B. System Architecture

The focus of this work is on a sub-Nyquist sampling receiver front-end, however several other pieces of equipment are required to demonstrate a full ultrasound system. Figure 3 illustrates the components surrounding the sub-Nyquist sampling AFE. The transmit pulses are produced by a Verasonics machine (Verasonics, Inc., Redmond, WA). A Philips ATL L7-4 128-element linear array probe is used. The probe has been spliced into a breakout board; this allows for the Verasonics machine to drive the array during transmit, while allowing for simultaneous receive operation by both the Verasonics imager as well as by our sub-Nyquist sampling AFE. This testing architecture allows for a performance comparison between a conventional Verasonics ultrasound machine and our sub-Nyquist sampling AFE.

The sampling and digitization functionality is provided by a National Instruments PXI-5105 8-channel ADC (National Instruments, Austin, TX). The ADC is triggered by a ML605 demonstration board, featuring a Virtex 6 FPGA (Xilinx, Inc., San Jose, CA). This Virtex 6 FPGA also provides the VGA gain control as well as the 64 phased mixing signals used for the subarray beamforming. Using MATLAB (The Mathworks Inc., Natick, MA), this low-rate sampled data is beamformed in the frequency-domain as in [6-8] before being reconstructed using the NESTA algorithm [10].

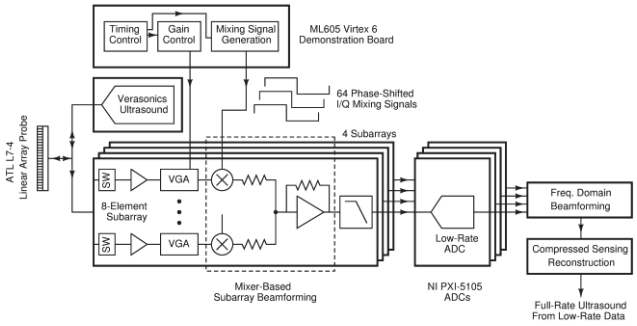

Figure 3: System architecture for sub-Nyquist sampling AFE. Transmit operation is controlled by the Verasonics machine. Reflected signals are received simultaneously by the Verasonics and sub-Nyquist AFEs.

C. Test Conditions

The Verasonics machine was programmed for B-mode imaging with a linear array. During the transmit operation, a 4.5 MHz single cycle 40 V pulse is used. All 128 elements of the Philips ATL L7-4 linear array probe were used during the transmit phase, beamformed to a depth of 5.1 cm into the target. A Gammex RMI 406 (Gammex, Inc., Middleton, WI) phantom was used as the test target.

During the receive operation, each receiver processes signals from the center 32 elements of the transducer array. This 32 channel limitation is imposed by the channel count of the available digitizer equipment; it is crucial to note that the techniques demonstrated here are not limited either by transducer count or imaging geometry.

III. Mixer-Based Subarray Beamforming

The narrowband nature of the sub-Nyquist sampling approach allows us to use dynamically changing phase shifts in our mixing signals to implement the dynamic time shifts between elements required for subarray beamforming [9]. The 64 required mixing signals (in-phase and quadrature for each of the 32 channels) were calculated *a priori* given the known geometry of the 97 received scanlines.

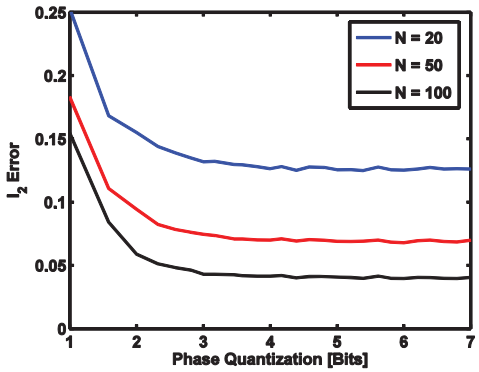

Figure 4: Simulated characterization of phase quantization on reconstruction accuracy. While overall beamforming accuracy is dictated by the number of samples taken for frequency-domain beamforming, error introduced by phase quantization is limited after 4 bits.

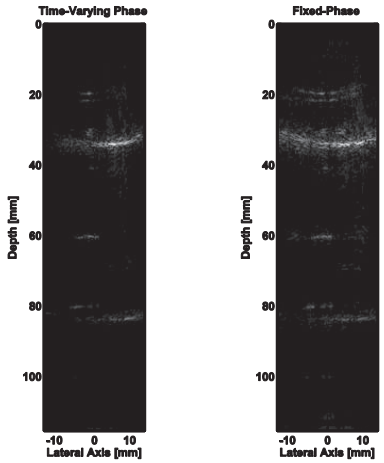

Figure 5: Images reconstructed from low-rate samples measured with the sub-Nyquist sampling AFE. Figure (a) implements subarray beamforming using time-varying phase in the mixing signals as in [9], (b) uses fixed-phase mixing sequences instead.

The Virtex 6 FPGA uses a 100 MHz clock, producing mixing signals with a fundamental frequency of 4.16 MHz and phase quantization to 24 levels. To verify that this phase quantization yielded acceptable performance, a synthetic scanline was generated in MATLAB and sampled at a rate of 250 MHz. The performance of our sub-Nyquist architecture was simulated using this synthetic input signal for 96 elements of pitch 298 μm, with subarrays of 8 elements. Figure 4 shows the l_2 error between the signal reconstructed from low-rate samples (as a function of phase quantization) and the conventionally beamformed signal using the full-rate input. Each sub-Nyquist reconstruction was made from 201 samples, with 20, 50, and 100 additional samples used for frequency-domain beamforming [6-7]. While the minimum error magnitude depends on the number of samples taken for the frequency-domain beamforming step, phase resolution beyond 4 bits (16 levels) provides little additional benefit.

Figure 5 shows measured performance of the sub-Nyquist AFE when (a) the mixers employ subarray beamforming signals, and (b) when the time-varying phase delay are set to 0 (no delays are implemented before subarray summation). It is clear from this data that using mixer-based subarray beamforming provides a benefit to image quality, especially in the foreground of the image. The image quality can be quantitatively compared between these images with the SSIM [11]. The SSIM provides a similarity comparison between a reference image and another image in question; this metric is considered to be more perceptually accurate than absolute measures such as mean-squared error (MSE). When compared to the full-rate time-domain beamformed signal (not shown), the reconstructed images in Figure 5 have SSIM metrics as shown in Table I. The measured values for SSIM demonstrate good agreement with the SSIM values from the prior simulation work in [7] and [9].

TABLE I. EFFECT OF MIXER-BASED SUBARRAY BEAMFORMING

Subarray Beamforming Signals	*SSIM*	*NRMSE*
Time-Varying Phase Mixing Signals (Fig. 5a)	0.7568	0.0964
Fixed-Phase Mixing Signals (Fig. 5b)	0.5979	0.1161

IV. RECONSTRUCTED IMAGE QUALITY

Finally, we compare performance between the sub-Nyquist sampling AFE and the Verasonics machine. 97 scanlines are recorded, with a horizontal spacing of 298 μm. With the Verasonics imager, 2700 samples were taken per channel at a rate of 18 MS/s for a maximum imaging depth of 11.5 cm. With the sub-Nyquist sampling AFE, 200 samples were used for CS reconstruction, with an additional 50 samples for frequency-domain beamforming as in [7]. With a subarray size of 8, this results in a factor of 43x less data than used by the Verasonics imager. A 2nd order Butterworth filter with cutoff frequency of 625 kHz was used as the low-pass filter. Figure 6 compares the image produced by the Verasonics machine when sampled at full-rate (a) against the simulated performance of the sub-Nyquist sampling AFE (b) from this full-rate data. Also shown is the reconstructed image resulting from measured samples from the PCB sub-Nyquist sampling AFE (c). Timing and VGA gain characteristics were calibrated between the Verasonics and sub-Nyquist receivers. Comparing the reconstructions resulting from the low-rate measured data and the low-rate simulated data against the full-rate Verasonics data results in the SSIM and NRMSE values presented in Table II.

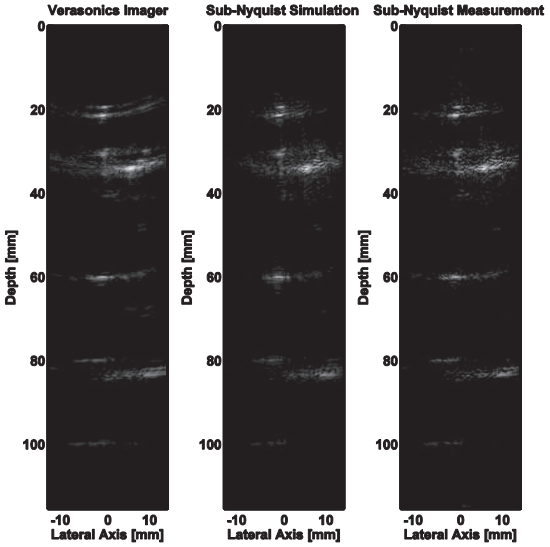

Figure 6: Comparison between a conventional full-rate beamformed image (a) and the simulated sub-Nyquist AFE performance given measured full-rate data (b). Image (c) is the measured sub-Nyquist AFE reconstruction from the same transmit event. Images (b) and (c) were generated using a factor of 43 less data than image (a).

TABLE II: RECONSTRUCTED IMAGE QUALITY

Image	*SSIM*	*NRMSE*
Sub-Nyquist AFE Measurement	0.7692	0.0896
Sub-Nyquist AFE Simulation	0.7686	0.0813

When designing a sub-Nyquist sampling AFE, there is an inherent tradeoff between the number of samples taken (and thus the overall data rate) and the resulting reconstruction accuracy. To test the reconstruction accuracy of the sub-Nyquist AFE as a function of sample count, we use a high sampling rate of 60 MS/s on the NI PXI-5105. The sampled data from the sub-Nyquist hardware is downsampled prior to frequency-domain beamforming and the subsequent CS reconstruction. Figure 7 characterizes the SSIM of the low-rate reconstructed image against the full-rate conventionally beamformed image as a function of the number of samples used for CS reconstruction. For this experiment, a subarray size of 8 was used for the mixer-based beamforming, with 50 additional samples taken for frequency-domain beamforming. The blue curve presents the SSIM between the reconstruction from the sub-Nyquist AFE samples and the Verasonics box, and the red curve shows the SSIM between the simulated AFE performance and the Verasonics full-rate image. The black curve represents the SSIM between the simulated performance and the measured performance of the sub-Nyquist AFE. The measured reconstruction demonstrates a high degree of accuracy when compared to simulation.

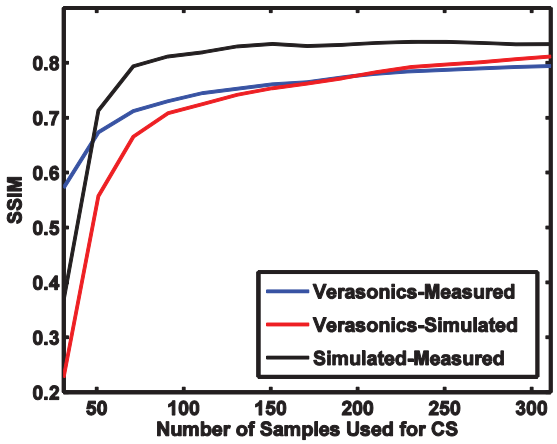

Figure 7: Characterization of sample count on the resulting reconstructed image SSIM when compared against a full-rate signal. A smooth tradeoff exists between sample count and image accuracy, and a high level of agreement is found between the reconstructions from simulation and measured data.

V. CONCLUSION

This paper described a hardware demonstration of a sub-Nyquist sampling AFE for B-mode ultrasound imaging. By digitizing only a fraction of the physical bandwidth, the overall data rate can be reduced by more than a factor of 40. The reduction is achieved through a combination of sub-Nyquist sampling and subarray beamforming. Our measurements confirmed that the sub-Nyquist system maintains high image quality.

REFERENCES

[1] S.W. Smith, Jr. Pavy, H.G., and O.T. Von Ramm, "High-speed ultrasonic volumetric imaging system. i. transducer design and beam steering." *Ultrasonics, Ferroelectrics, and Frequency Control*, *IEEE Transactions on*, vol. 38, no 2, pp. 100-108, March 1991.

[2] A. Bhuyan, J.W. Choe, B.C. Lee, I. Wygant, A. Nikoozadeh, O. Oralkan, B.T. Khuri-Yakub, "Integrated Circuits for Volumetric Ultrasound Imaging with 2-D CMUT Arrays," *Biomedical Cicuits and Systems, IEEE Transactions on*, vol. 7, no. 6, pp. 796-804, 2013.

[3] M. Karaman, I. Wygant, Oralkan, O., B.T. Khuri-Yakub, "Minimally Redundant 2-D Array Designs for 3-D Medical Ultrasound Imaging,", *Medical Imaging, IEEE Transactions on*, vol. 28, no. 7, pp. 1051-1061, 2009.

[4] A. Austeng, S. Holm, "Sparse 2-D Arrays for 3-D Phased Array Imaging – Design Method," *Ultrasonics, Ferroelectrics, and Frequency Control, IEEE Transactions on,* vol. 49, no. 8, pp. 1073-1086, 2002.

[5] R. Tur, Y.C. Eldar, and Z. Friedman, "Innovation rate sampling of pulse streams with application to ultrasound imaging," *Signal Processing, IEEE Transactions on*, vol. 59, no. 4, pp. 1827-1842, April 2011.

[6] N. Wagner, Y.C. Eldar, and Z. Friedman, "Compressed beamforming in ultrasound imaging," *Signal Processing, IEEE Transactions on,* vol. 60, no. 9, pp. 4643-4657, Sept. 2012.

[7] T. Chernyakova and Y.C. Eldar, "Fourier-domain beamforming: the path to compressed ultrasound imaging," *Ultrasonics, Ferroelectrics, and Frequency Control, IEEE Transactions on,* vol. 61, no. 8, pp. 1252-1267, August 2014.

[8] Y.C. Eldar, "Sampling Theory: Beyond Bandlimited Systems," Cambridge University Press, April 2015.

[9] J. Spaulding, Y.C. Eldar, and B. Murmann, "Mixer-Based Subarray Beamforming for Sub-Nyquist Sampling Ultrasound Architectures," *Proc. ICASSP*, Brisbane, Australia, Apr. 2015, pp. 882-886.

[10] S. Becker, J., Bobin, E., Candes, "NESTA: a Fast and Accurate First-Order Method for Sparse Recovery," *SIAM Journal on Imaging Sciences*, 2007.

[11] Z. Wang, A., Bovik, H. Sheikh, E. Simoncelli, "Image Quality Assessment: From Error Visibility to Structural Similarity," *Image Processing, IEEE Transactions on*, 2004.